

# Study On Parameter Optimization of 3D Bioprinting of Hybrid Bio-Inks

Sagil James (✉ [sagiljames@fullerton.edu](mailto:sagiljames@fullerton.edu))

California State University Fullerton College of Engineering and Computer Science

<https://orcid.org/0000-0003-2570-2968>

Samir Mulgaonkar

California State University Fullerton

---

## Research Article

**Keywords:** Bioprinting, Additive Manufacturing, Scaffold, Alginate

**Posted Date:** August 31st, 2021

**DOI:** <https://doi.org/10.21203/rs.3.rs-836634/v1>

**License:** © ⓘ This work is licensed under a Creative Commons Attribution 4.0 International License.

[Read Full License](#)

---

**Version of Record:** A version of this preprint was published at The International Journal of Advanced Manufacturing Technology on January 23rd, 2022. See the published version at <https://doi.org/10.1007/s00170-021-08561-7>.

# Abstract

Used mainly for manufacturing operative tissue structures to replace damaged ones, Three-dimensional (3D) Bioprinting is a burgeoning area of medical science with enormous potential. Since the technology is still relatively new, 3D bioprinting heavily relies on the trial-and-error approach for advancement, but the general process currently involves a mixture of various biomaterials in hydrogel form. The quality of the results is affected significantly by the parameters by which the print is made. Even the most seemingly minute details can drastically change the outcome of the print, including temperature, print time, the speed of the occurring print and nozzle diameter, dispensing pressure, and more. The biomaterial used is also of the utmost importance. Based on current results, an ideal biomaterial should include the same or similar chemical, biological, mechanical, and practical properties of the target end structure. It is critical to ascertain the closest parameters available to ensure a quality end resulting print. The proposed studies' goal is to determine and streamline process parameters to the nearest possible degree to optimize the bioprinting process of hybrid bioinks. Using material made from unchanged alginate, alginate with gelatin, and combined amino acids and derivatives with diphenylalanine, the medical properties of each biomaterial were examined, as well as their flow behavior, allowing a certain level of predictability on printing parameters. Printing parameters, as described, are the parameters by which we can predict how well a target structure can be accurately constructed using various bio-inks. Ultimately, the results have indicated that printing parameters primarily hinges on the composition of the hydrogels used and the pressure by which it was distributed. This study also presented a detailed frame of reference to assess amino acids and derivatives with diphenylalanine systematically, which can also be used in other areas of 3D bioprinting.

# Introduction

Additive manufacturing has several different methods, and one of them is the extrusion type shown in Fig. 1 that has gained popularity in bioprinting for tissue construction applications [1]. Several studies have revolved around the creation of hydrogel scaffolds using this kind of printing [2, 3]. For the most part, Three-dimensional (3D) reconstructed computer-aided designs (CAD) models form the basis of depositing the biomaterials [4]. In general, scaffolds prove challenging to reproduce to scale utilizing the CAD models, which is why it can be so critical to determining printing parameters before construction. Three-dimensional (3D) printing parameters using a biomaterial compound in hydrogel form are often described as the ability and reliability of that material to form and maintain a 3D structure that is both sound and reproducible.

These overall printing parameters can profoundly influence other seemingly related factors, like the mechanical characteristics of the printed outcome and the morphology of the scaffolds produced. This, consequently, means that printing parameters influence all cell responses [5]. With this in mind, it is vital to determine and study elements that can affect printing parameters.

This study focuses on extrusion-based three-dimensional (3D) bioprinting of hybrid bioinks and a few critical challenges in this field known as printing parameters. The aim is to isolate and discuss potential factors that can alter printing parameters and identify methods of measurement for it, specifically concerning the printing parameters of hydrogel scaffolds. As it stands, the flow of behavior in biomaterials has been studied, paying particular attention to factors like ink consistency [6, 7], the characteristics of the biomaterials involved [8], the mechanical aspects of varying hydrogel compounds [9], and the desired outcome. Despite this, not enough is currently known to draw consistent conclusions regarding the specifics of specialized printing. As a result, the needed parameters for printing scaffolds from a concoction comprised of hydrogels and other biomaterials have yet to be identified. Not enough consideration has been given to printing features that can affect scaffolds made from hydrogel compounds [2]. This study pertains to this issue, and it includes changes in mechanical properties, degeneration, and enlargement over time based on the hydrogel mixture used, including the compounds alginate, alginate-gelatin, alginate-diphenylalanine, and alginate-gelatin-diphenylalanine. This study systematically implements characterizations by which the material flow behavior can be documented, based on both 2D and 3D printing parameters of various hydrogel compounds. These findings are then mapped out to illustrate the relationship between fabricated materials and biomaterials and how they affect printing parameters.

While some studies on the effects of various biomaterials and their printing parameters exist, a clear, definite understanding and ubiquitous definition of printing parameters remain elusive. A basic question like how to explore the connection between other crucial properties that affect printing parameters remains unanswered. A few studies where the flow pattern of particular biomaterials was used to evaluate and determine printing parameters prove to be an example of this [6, 7]. In these studies, the rheological and physical characteristics of the material were the focus of investigation without consideration of other factors [9], whereas in another study, the only factor considered was the effect of ionic cross-linkers [10]. Some studies went on to focus exclusively on printing parameters and their effect on printing parameters [2, 11]. One study focused on the gelation characteristics during the printing stage to map a structurally and mechanically sound print [12]. Another study focused on gelation factors, enlargement, and the overall printing parameters of varying hydrogel compounds [13]. A separate study, endeavoring to check the analytical methods used, details the printing parameters of materials based on compounds that were analyzed [14]. Kyle et al. went on to report that printing parameters are essentially a matter of rheology, nozzle, and printing parameters like filament and pore dimensions, a geometry which may include the printing angles, and biomaterial composition [15]. Armed with this information, it is clear that considering only one factor in printing parameters while disregarding others is not an effective approach to improving the understanding and practical applications of printing parameters. As indicated, several research studies have analyzed the individual effects on printing parameters and have made small strides to understand the topic further. A clear perception of printing parameters that considers the inter-related conditions which influence it does not currently exist. Rather than focusing on each conditional change exclusively, this study analyzed printing parameters, printing conditions, and rheological properties in detail to systematically map the relationship between printing parameters and

the factors that can affect them. As understanding develops, it is crucial to perform more and further in-depth studies to more accurately describe and affirm innovative ways to measure printing parameters. How to measure printing parameters is the critical question and focus of this study [15].

Alginate is known as one of the few hydrogel compounds used in the bio-manufacturing of scaffolds that are used in tissue construction applications, as recorded in several performed studies [16–23]. A common strategy currently used to refine printing parameters of alginate-based scaffolds', specifically ones constructed using extrusion-based printing, is to blend the pure alginate and some form of hydrogel compounds [24]. Gelatin is specifically combined with alginate, as it is a natural, collagen-derived polymer. Gelatin is considered a cell-friendly environment, making it ideal for mixing this way [12]. Amino acid and amino acid derivatives are compounds that contain both carboxyl and amino types, which prove useful in varying types of peptidomimetic and peptide synthesis [25]. Alternatively, diphenylalanine is either naturally occurring or chemically synthesized amino acids that are non-proteinogenic. Due to a wide range of structural diversity and functionality, these compounds are widely used as building blocks in developing combined libraries. A choice study investigated the characteristics of some cell substrates comprised of natural and chemically synthesized amino acids. The results indicated that the scaffolds with higher water retention rates generally have both of these properties [8]. This ultimately proves that mixing various materials can be one way to control the resulting outcome of the scaffold finely, thus allowing better control over desired functions.

## Methods

### 2.1. Hydrogel Preparation

For the preparation of hydrogels, sodium alginate ( $C_6H_9NaO_7$ ) with a medium viscosity, gelatin made from porcine skin, Type A, Bioreagent, diphenylalanine, and naturally occurring amino acids were used as shown in Table 1. These materials were specifically selected since they are the most popularly used materials in the current 3D bioprinting applications.

Table 1  
Types of hydrogel formulations used in this study

Type	w/v Sodium alginate	w/v of other materials
1	5.0 %	None
2	3.0 %	2.0 % w/v pure gelatin
3	3.0 %	2.0 % w/v Fmoc-Phe-Phe-OH
4	2.0 %	1.50 % Fmoc-Phe-Phe-OH 1.50 % w/v Fmoc-Ser-OH
5	2.0 %	1.50 % w/v pure gelatin, 1.50 % w/v Fmoc-Phe-Phe-OH- Diphenylalanine
6	2.0 %	1.0 % w/v pure gelatin, 1.0 % Fmoc-Phe-Phe-OH 1.0 % w/v Fmoc-Ser-OH

In order to ensure a uniform mix for printing, vortex mixing was used to prepare the solutions. The mixed compound was then centrifuged to ensure the removal of bubbles and refrigerated for complete hydration. The solutions were then kept in an extruder syringe for 30 minutes prior to the printing process.

## 2.2. Fabrication of the Scaffold

In the printing process, a three extruder Bioprinter (make: Allevi Inc., model: Allevi 3) was selected for scaffold construction, and the hydrogels were dispensed using varying gauges of the needle. The Allevi Bioprint software aided in slicing, and the scaffolds were constructed with series of layers one by one while hydrogel extrusion was immersed in a calcium chloride bath in a separate petri dish. All parameters of the scaffold were measured and documented using the ImageJ software, including pore sizes and area, the filament width, and the perimeter of the completed scaffold. The prints were completed three times using three different extruders to ensure uniformity and the desired outcome.

## 2.3. Enlargement Properties of Hydrogel

The beginning weight of the scaffolds was measured and documented after removing them from the printing solution and then brooded in a Phosphate-buffered saline solution at 37°C. The specimen was then weighed again periodically after 1.0 hour, 3.0 hours, 12.0 hours, 24.0 hours, 72.0 hours, 144.0 hours, and 168.0 hours for any change which would be attributed to due to exchange of moisture between the scaffold and Phosphate-buffered saline. The enlargement was described utilizing the following equation:

$$\% \text{ Enlargement} = \left( \frac{w_f - w_i}{w_i} \right) \times 100 \quad (1)$$

where,  $w_i$  is the initial weight and  $w_f$  is the final weight.

## 2.4. Deformation Strength

The resulting scaffolds were then tested for deformation stability using a tensile tester (make: Mark-10, model: M3-100), which measures the force required to deform a specimen to varying degrees of displacement until a maximum of 1.0 mm is reached. This test also measured and documented the resulting area and height of the scaffolds, so this information could be utilized to map a load-displacement (SN) curve for individual scaffold, and resulting tensile modulus were obtained.

## 2.5. Degeneration Properties of Hybrid-Hydrogel

First, the constructed scaffold models were frozen, weighed, and documented to obtain initial mass. To procure the degenerated samples, scaffolds were brooded in Phosphate-buffered saline at 37°C for 2.0, 4.0, and 7.0 days. Phosphate-buffered saline solution was then removed from the samples, which were frozen and then weighed again. The degeneration of the hydrogel compounds was obtained with the following equation:

$$\% \text{ Degeneration} = \left( \frac{w_f - w_i}{w_i} \right) \times 100 \quad (2)$$

where,  $w_i$  is the initial weight and  $w_f$  is the final weight.

## 2.6. Studies of Printability Evaluations and Conditions

For verifying the two-dimensional experiment known as 2D, three layers were printed. More studies were performed to verify the 3D culpability of these results based on different types. In the following subsections, the design remains an experimental guideline on evaluating the effects of pattern selection, air pressure, and nozzle speed.

### 2.6.1. Compressor Air Pressure

For this experiment, air pressure from 1.0 psi to 6.0 psi and temperature 37.0°C, 42.0°C, and 50.0°C were subjected to change while the nozzle speed was maintained in a constant state and deviation in the Y direction was measured to see the distortion from the actual CAD strand diameter.

### 2.6.2. Nozzle Speed

The second experiment involves a change in nozzle speed, from 6.0 mm per second to 35.0 mm per second. The results here were also influenced by the best pressure from the previously established air pressure experiment, which was carried on 10.0 mm x 10.0 mm x 3.0 mm. The temperature here was kept at a constant 37.0°C, and the needle size stayed at the 23 gauge.

### 2.6.3. Pattern Printing

The study involves the investigation of 4 different angular patterns, including 25°, 45°, 90°, and finally 130°. Pressure, nozzle speed, and temperature were kept constant at between 1.0 psi (0.05 bar) and 6.0

psi (0.4 bar), 15.0 mm per second to 35.0 mm per second and 37.0°C, respectively.

## **2.7 Printing parameters Evaluation**

This study performed several different evaluations to provide methods of measuring printing parameters. This study used four general needle sizes, which include 30G, 28G, 25G, and 23G. The strand diameter, while experimental, was compared to the needle inner diameter for ranging in speed anywhere between 6.0 mm and 35.0 mm per second while temperature stayed constant. Experiments were done and redone in weeks 1 and 2 to evaluate the relative connection of biomaterial degeneration and strand diameter.

## **Results And Discussion**

### **3.1. Enlargement, Degeneration, and Mechanical Properties**

The studies indicate that the enlargement properties of biomaterial compounds are directly related to the ability of wastes and nutrients to be redistributed and interchanged between the local environment and the cells, which are meant to be integrated into the hydrogels for synthetic production and its use. All of the specimens collected in this research were brooded to analyze and identify how fast the water was retained with time, and mass occupied due to this retention are seen in Fig. 2.

In short, Type 1 showed an overall enlargement of 200.0 %, Type 2 indicated a 250.0 % enlargement over the same amount of time, Type 3 showed a 275.0 %, Type 4 displayed a 400.0 %, Type 5, 350.0 %, and Type 6, 325.0 % enlargement after the 144th hour of incubation with PBS. As revealed by this information, Type 4 and the hybrid used displayed the greatest rate of water retention and the largest modification of mass occupied with time. Degeneration was then analyzed for each specimen. Type 1, 2, 3, 4, 5, and 6 showed a 35.0 %, 22.0 %, 33.0 %, 37.0 %, 15.0 % and 18.0 % degeneration overtime respectively. Deformation strength in all participating types was ultimately determined by finding, documenting, and comparing tensile modulus of each Type as depicted in Fig. 3 on a weekly basis.

The tensile strength of Type 1 samples was 14.0 psi (95.57 kPa), 9.0 psi (60.8 kPa), while Type 2 samples were 11.0 psi (73.4 kPa), 5.0 (36.3 kPa). The results for Type 3 samples were 12 psi (82.67 kPa), 5.0 psi (33.55 kPa). Type 4 samples were 15.0 psi (98.7 kPa), 6.0 psi (41.45 kPa). Type 5: 11.0 psi (75.9 kPa), 6.0 psi (40.8 kPa), and Type 6: 10.0 psi (70.56 kPa), 5.0 psi (31.86 kPa). Week two specimen was measured after brooding in phosphate buffer saline. These results indicate that there was a decline in the deformation strength of each of the hydrogel compounds. In addition to this finding, these results show that the Type 4's scaffolds have the highest tensile stress in comparison to the other hybrid hydrogels.

### **3.2. Effect of Printing Properties**

#### **3.2.1. Pressure Variation Test**

Decidedly one of the most critical factors in printing parameters is air pressure [2]. As it is understood, every biomaterial should have extrusion pressure that exceeds the surface pressure of that material.

Figure 4 illustrates how the change in pressure effect prints and also shows purging statuses on types 1–6 at varying temperatures (37.0°C, 42.0°C, and 50.0°C). For some specimen, as indicated in the graph, printing was just not a viable option. Higher pressures made extruded biomaterial unstable in some of these samples and resulted in poor printing parameters. Type 1 acted as a non-viscous material. Type 2 had viscous behavior but proved unprintable. Type 3 through Type 6 showed properties that can be described as viscous, and results revealed that 3.0 psi (0.2 bar) was a sufficient pressure level to print with.

### **3.2.2. Extrusion Nozzle Speed Test**

In this experiment set, the extrusion nozzle operating speed was changed and documented based on the sample type. Figure 5 shows the different results for the different sample types with a comparison to the CAD models. Results here show that deviation in the X and Y do not specifically depend on nozzle speed. In short, the average deviation in all types was noted as 0.5 mm across all speeds.

### **3.3. Printing Angular Patterns**

Samples including angles of varying degrees, including acute, right, and obtuse, were printed (Fig. 6). Table 2 describes the relationship to the CAD model and the generalized measured angle for each nit in each type. The printing parameters here show that not all types produced a good angle for printing parameters. The quality became worse with right angles, so much so that scaffolds printed with a 0–90-degree pattern were drastically reduced in quality when compared to the 0-25-degree angles. Obtuse angles showed little deviation.

Table 2  
 Comparison of CAD angles and the measured angles for each type of hydrogel at a fixed set of CAD angle measurements (25°, 45°, 90°, 130°).

Hydrogel Types	CAD design angle (°)	Measured angle (°)
1	25	25.6 ± 0.2
	45	45.3 ± 0.2
	90	90.9 ± 0.2
	130	130.6 ± 0.2
2	25	25.6 ± 0.2
	45	45.2 ± 0.2
	90	91.0 ± 0.2
	130	130.6 ± 0.2
3	25	25.7 ± 0.2
	45	45.8 ± 0.2
	90	91.1 ± 0.2
	130	130.3 ± 0.2
4	25	25.6 ± 0.2
	45	45.2 ± 0.2
	90	90.8 ± 0.2
	130	130.4 ± 0.2
5	25	25.7 ± 0.2
	45	45.8 ± 0.2
	90	91.2 ± 0.2
	130	130.9 ± 0.2
6	25	25.3 ± 0.2
	45	45.6 ± 0.2
	90	90.9 ± 0.2
	130	130.4 ± 0.2

### 3.3.1. Printing parameters Evaluation

The experiment shows that the average X and Y direction deviation was 1.5 mm (Fig. 7 and Fig. 8). It is also concluded that changing speed does not really affect deviation too much, but it was noted that as speed increases, the deviation reduces a little bit. From the graphs, it is concluded that 20 mm/s is the ideal speed to control the deviation within 1.5 mm (Fig. 9).

## Conclusion

Hydrogel compounds are an incredibly valuable area of study for the fields of medical science and the biomedical industry in general. Because of the simplicity in which they can be prepared, and most importantly, their similarities to extracellular matrices of human tissues, these incredible biomaterials serve as a suitable environment for cells. This research focused on 3D bioprinting of hybrid bioinks and investigated the enlargement, degeneration rate, and mechanical properties of biomaterial compounds with varying hydrogels consisting of alginate, gelatin, amino acids and its derivatives, and diphenylalanine. The results indicate composite hydrogels have an increased water retention capability when compared to a pure alginate compound. Furthermore, the elastic modulus decreased over time with all combinations of hydrogel, while the diphenylalanine combinations remained the highest. After assessing scaffolds from a mechanical perspective, follow-up studies considered more factors of hydrogel printing parameters. Results for these studies concluded that air pressure, nozzle speed, and diameter, as well as offset and angular pattern, all play roles in affecting printing quality. By systematically modulating these parameters, the printing parameters of different types of hydrogel compounds, which included alginate, gelatin, and diphenylalanine, were improved upon. Furthering research and conducting additional studies on printing parameters will allow for further improvement in and a deeper understanding of this area of medical science. More information in this field can lead to improvements in the technique of the construction and manufacturing of hydrogel scaffolds using the extrusion-based methods described. In conclusion, taking biomaterial and other construction essentials into serious consideration will improve printing parameters and allow for the specialization of scaffolds for the purposes of regenerative tissue therapy.

## Declarations

### a. Funding

The research team would like to acknowledge the support provided by Edwards Lifesciences, Irvine, CA. The facilities provided by the College of Engineering and Computer Science (ECS) at California State University Fullerton is also acknowledged.

### b. Conflicts of interest/Competing interests

The authors have no conflicts of interest to declare. All co-authors have seen and agree with the contents of the manuscript and there is no financial interest to report. We certify that the submission is original work and is not under review at any other publication.

### **c. Availability of data and material**

Not applicable

### **d. Code availability**

Not applicable

### **e. Ethics approval**

Not applicable

### **f. Consent to participate**

Not applicable

### **g. Consent for publication**

Not applicable

### **h. Authors' contributions**

Dr. Sagil James and Samir Mulgaonkar conceived the idea, designed the methodology and experimental set up, and outlined the paper. Samir conducted the literature review, performed experiments and collected data. Dr. James analyzed the data and wrote the results of the manuscript.

## **References**

1. Naghieh S et al., *Dispensing-based bioprinting of mechanically-functional hybrid scaffolds with vessel-like channels for tissue engineering applications—a brief review*. 2018. 78: p. 298–314
2. He Y et al., *Research on the printability of hydrogels in 3D bioprinting*. 2016. 6(1): p. 1–13
3. Naghieh S et al., *Influence of crosslinking on the mechanical behavior of 3D printed alginate scaffolds: Experimental and numerical approaches*. 2018. 80: p. 111–118
4. Skardal A and A.J.A.o.b.e. Atala, *Biomaterials for integration with 3-D bioprinting*. 2015. 43(3): p. 730–746
5. Ding H, R.C.J.A.S., Chang, *Printability study of bioprinted tubular structures using liquid hydrogel precursors in a support bath*. 2018. 8(3): p. 403
6. Chung JH et al., *Bio-ink properties and printability for extrusion printing living cells*. 2013. 1(7): p. 763–773
7. Ouyang L et al., *Effect of bioink properties on printability and cell viability for 3D bioplotting of embryonic stem cells*. 2016. 8(3): p. 035020
8. Pan T et al., *3D bioplotting of gelatin/alginate scaffolds for tissue engineering: influence of crosslinking degree and pore architecture on physicochemical properties*. 2016. 32(9): p. 889–900

9. Bertassoni LE et al., *Direct-write bioprinting of cell-laden methacrylated gelatin hydrogels*. 2014. 6(2): p. 024105
10. Sarker M et al., *Influence of ionic crosslinkers (Ca<sup>2+</sup>/Ba<sup>2+</sup>/Zn<sup>2+</sup>) on the mechanical and biological properties of 3D Bioplotted Hydrogel Scaffolds*. 2018. 29(10): p. 1126–1154
11. Sarker M et al., *Bio-fabrication of peptide-modified alginate scaffolds: Printability, mechanical stability and neurite outgrowth assessments*. 2019. 14: p. e00045
12. You F et al., *3D printing of porous alginate/gelatin hydrogel scaffolds and their mechanical property characterization*. 2017. 66(6): p. 299–306
13. Müller M et al., *Alginate sulfate–nanocellulose bioinks for cartilage bioprinting applications*. 2017. 45(1): p. 210–223
14. Gandhi JK, Opara EC (2013) and E.M.J.T.d. Brey. *Alginate-based strategies for therapeutic vascularization* 4(3):327–341
15. Freeman FE, D.J.J.S.r. Kelly, *Tuning alginate bioink stiffness and composition for controlled growth factor delivery and to spatially direct MSC fate within bioprinted tissues*. 2017. 7(1): p. 1–12
16. Ivanovska J et al., *Biofabrication of 3D alginate-based hydrogel for cancer research: comparison of cell spreading, viability, and adhesion characteristics of colorectal HCT116 tumor cells*. 2016. 22(7): p. 708–715
17. Bohari SP et al., *Effect of calcium alginate concentration on viability and proliferation of encapsulated fibroblasts*. 2011. 21(3): p. 159–170
18. Luo Y et al., *3D bioprinting scaffold using alginate/polyvinyl alcohol bioinks*. 2017. 189: p. 295–298
19. Ning L et al., *Influence of mechanical properties of alginate-based substrates on the performance of Schwann cells in culture*. 2016. 27(9): p. 898–915
20. Markstedt K et al., *3D bioprinting human chondrocytes with nanocellulose–alginate bioink for cartilage tissue engineering applications*. 2015. 16(5): p. 1489–1496
21. Gao T et al., *Optimization of gelatin–alginate composite bioink printability using rheological parameters: a systematic approach*. 2018. 10(3): p. 034106
22. Naghieh S et al., *Indirect 3D bioprinting and characterization of alginate scaffolds for potential nerve tissue engineering applications*. 2019. 93: p. 183–193
23. Lee S-H et al., *Analysis of degradation rate for dimensionless surface area of well-interconnected PCL scaffold via in-vitro accelerated degradation experiment*. 2014. 11(6): p. 446–452
24. Habib A et al., *3D printability of alginate-carboxymethyl cellulose hydrogel*. 2018. 11(3): p. 454
25. Ivanov C et al., *Synthesis of poly (vinyl alcohol): methyl cellulose hydrogel as possible scaffolds in tissue engineering*. 2007. 9(11): p. 3440–3444

## Figures

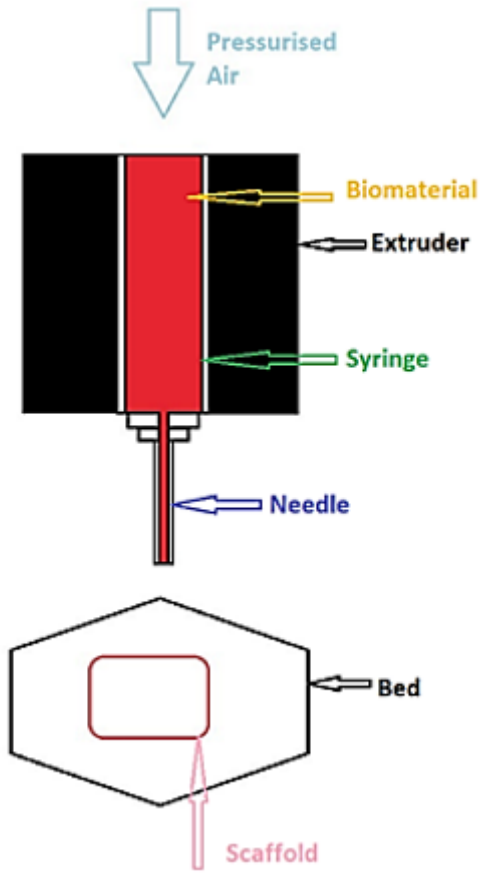


Figure 1

The process of bioprinting

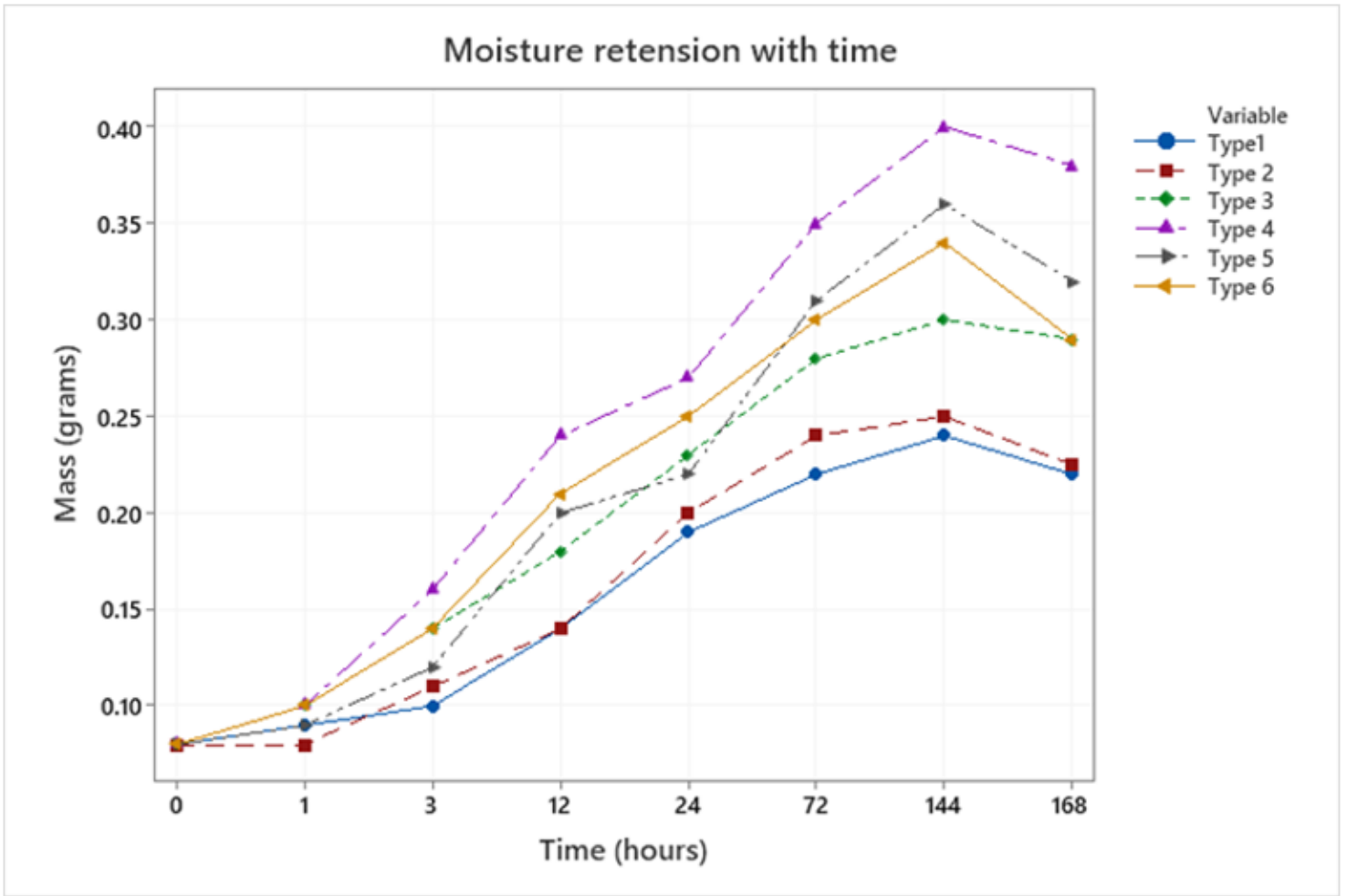


Figure 2

Time Series Plot of Type 1, Type 2, Type 3, Type 4, Type 5, and Type 6 about moisture retention in grams with respect to time

# Elastic Modulus of Different Types of Hydrogels

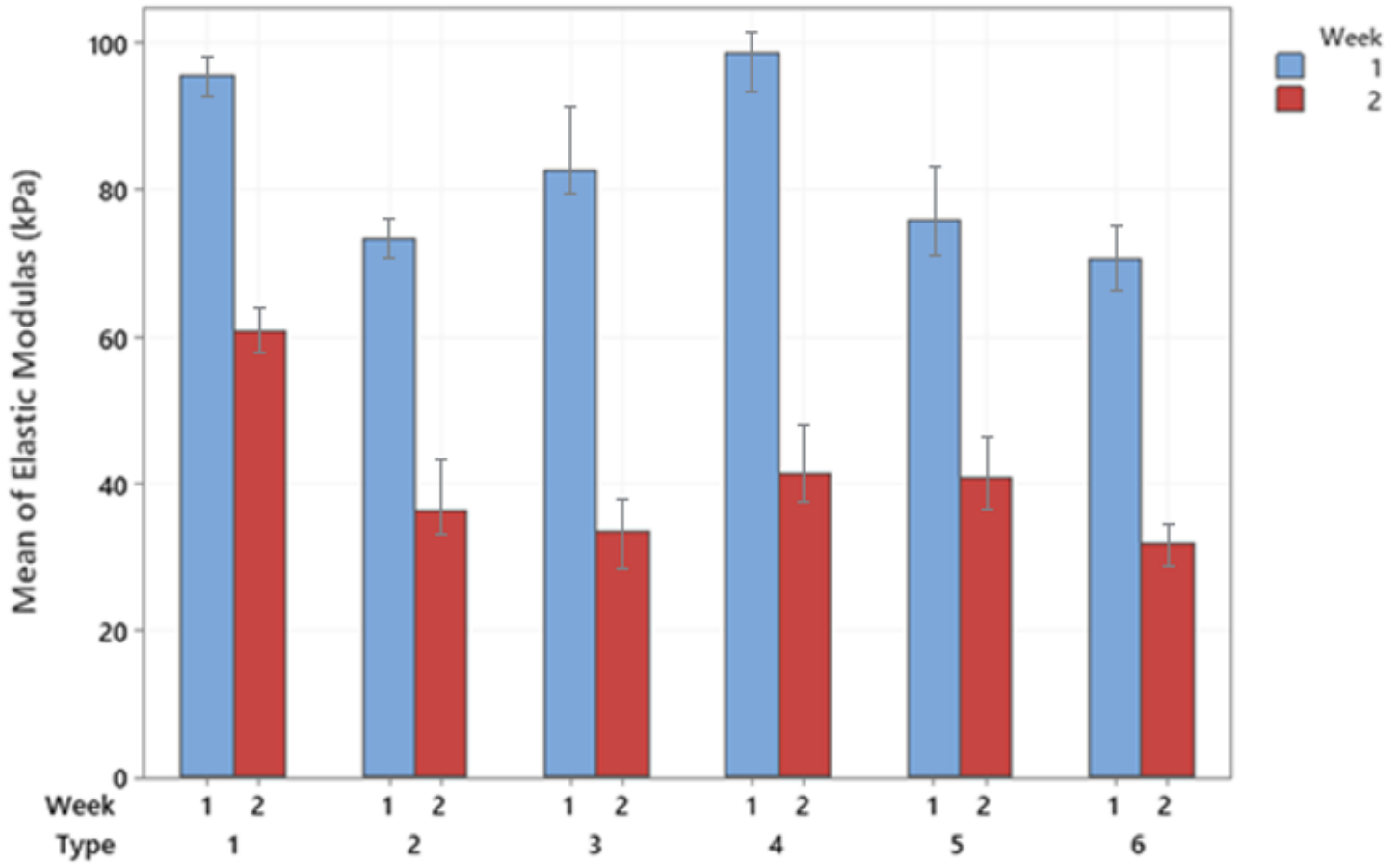
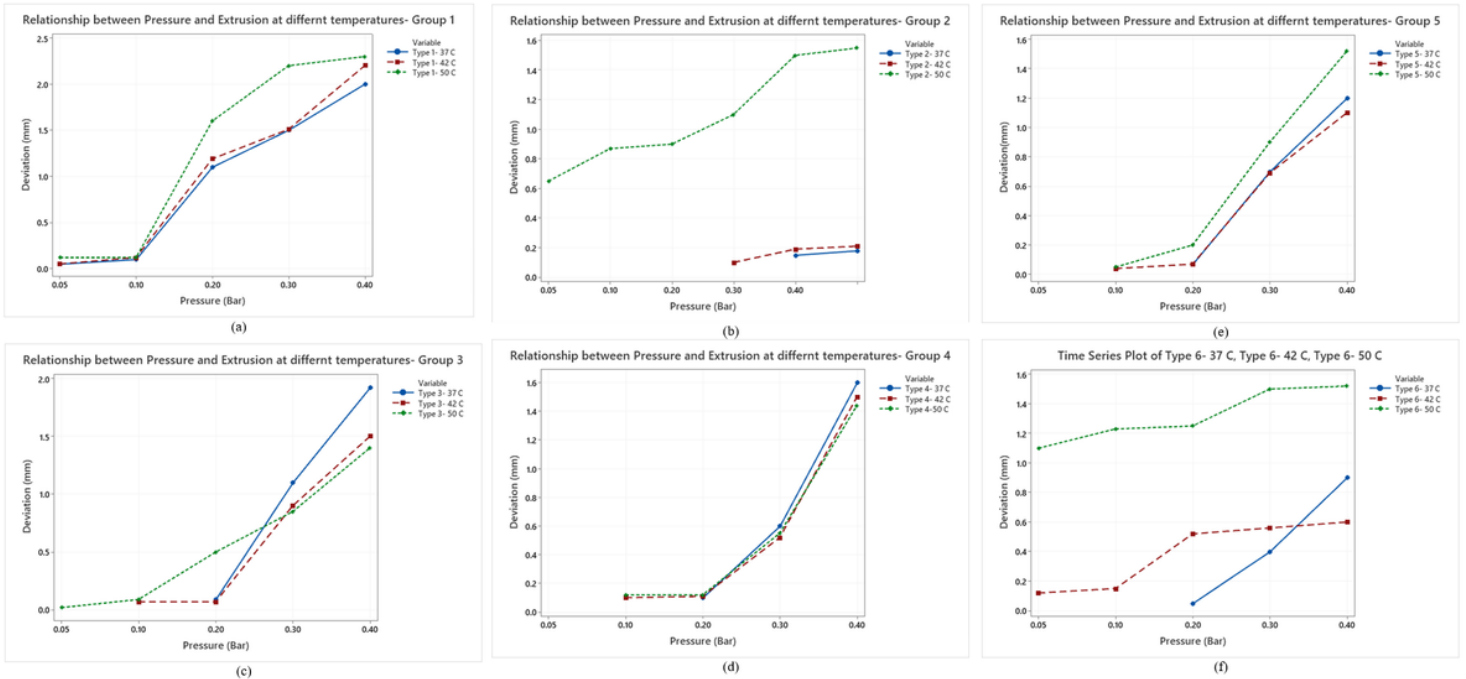


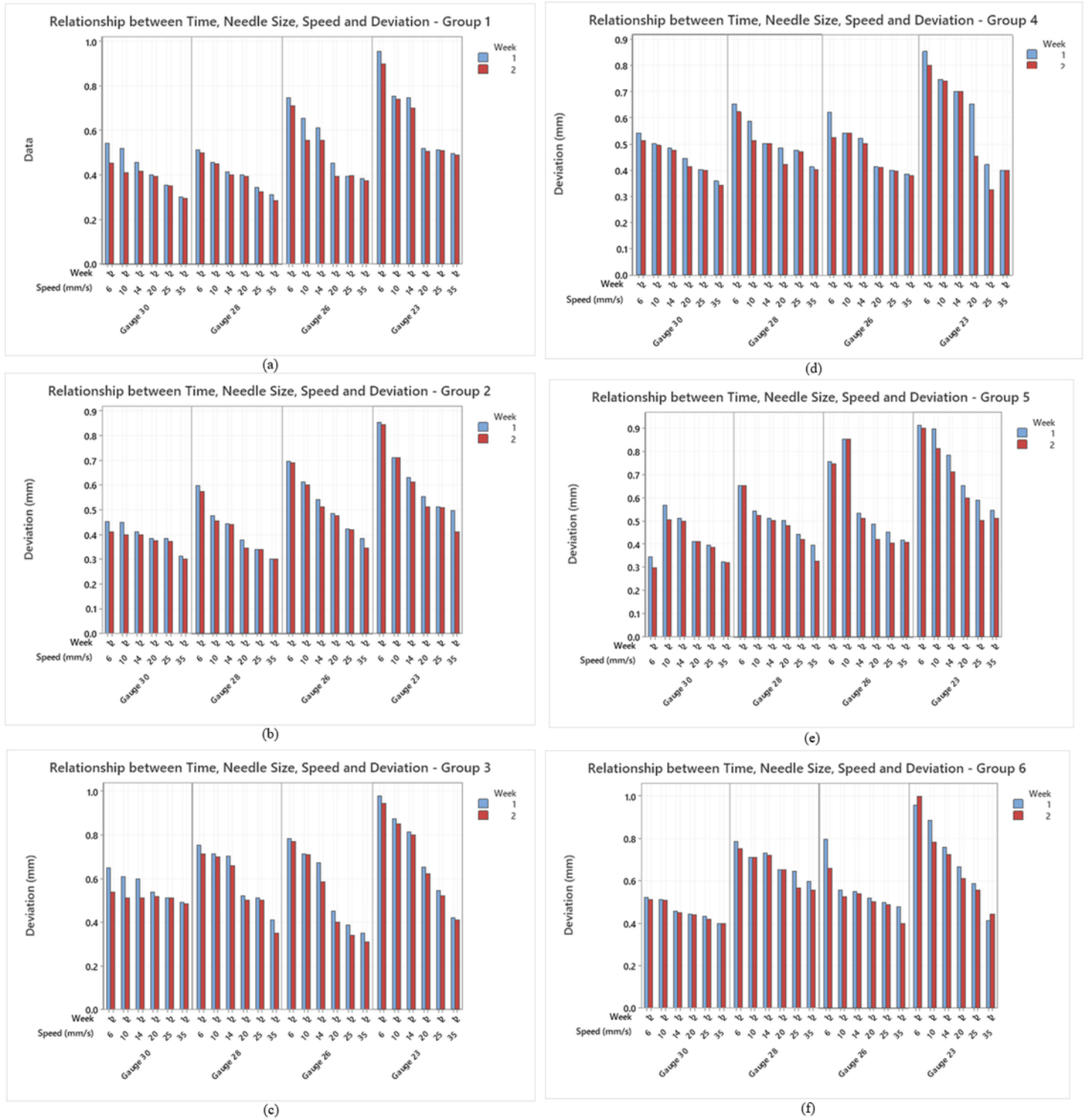
Figure 3

Chart of Mean (Elastic Modulus)



**Figure 4**

Relationship between Pressure and Extrusion at temperatures 37.0 °C, 42.0 °C and 50.0 °C for Types 1-6.  
 (a) Type 1 (b) Type 2 (c) Type 3 (d) Type 4 (e) Type 5 (f) Type 6



**Figure 5**

Relationship between Time, Needle Size, Speed, and Deviation over a period of two weeks is represented graphically for Types 1-6. The gauge sizes used for all Types are 30G, 28G, 26G, and 23G. (a) Type 1 (b) Type 2 (c) Type 3 (d) Type 4 (e) Type 5 (f) Type 6.

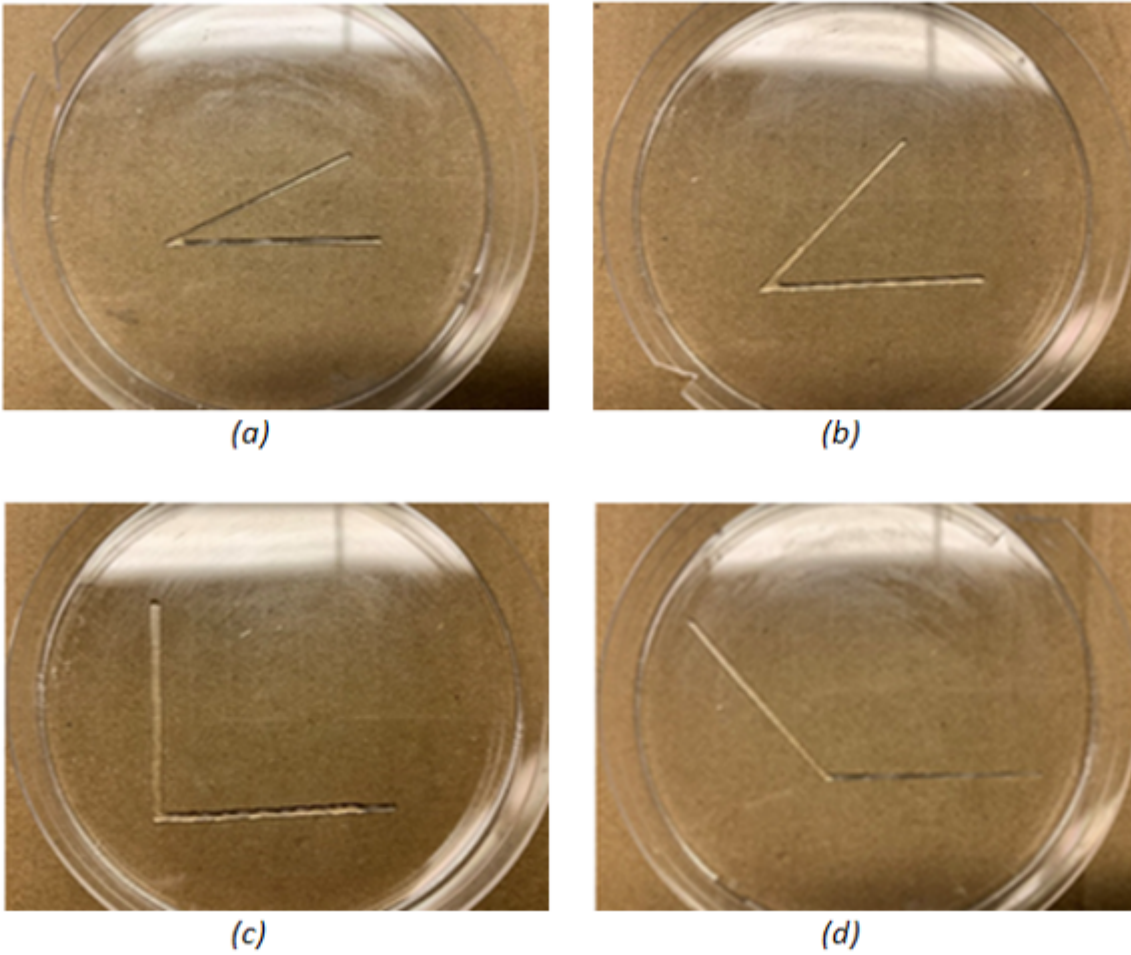
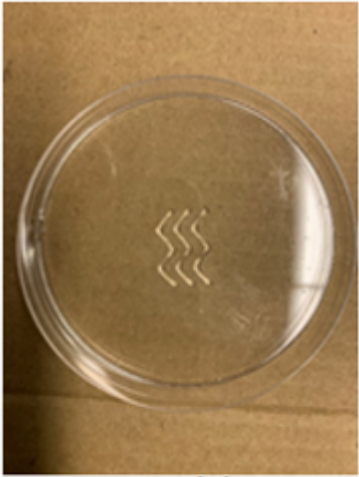
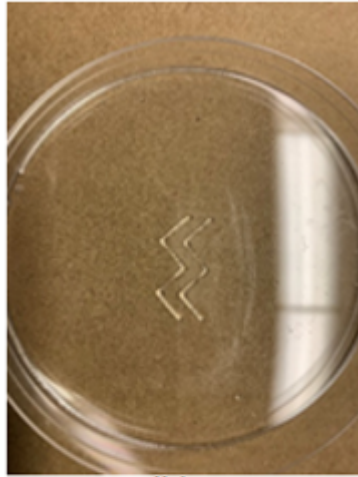


**Figure 6**

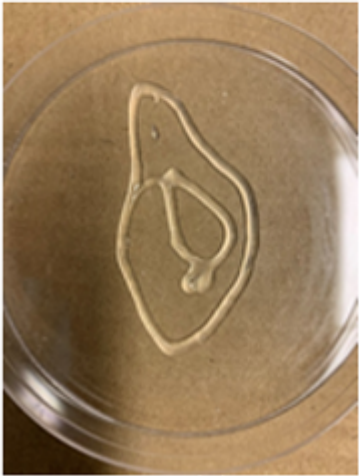
The angular printing patterns of varying angles: (a) 25° (b) 45° (c) 90° (d) 130°.



(a)



(b)



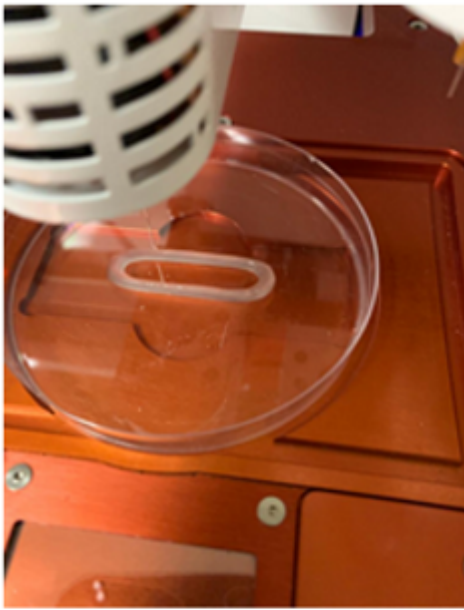
(c)



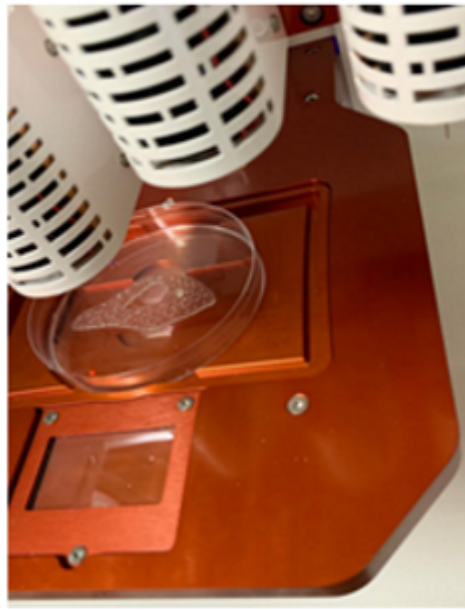
(d)

**Figure 7**

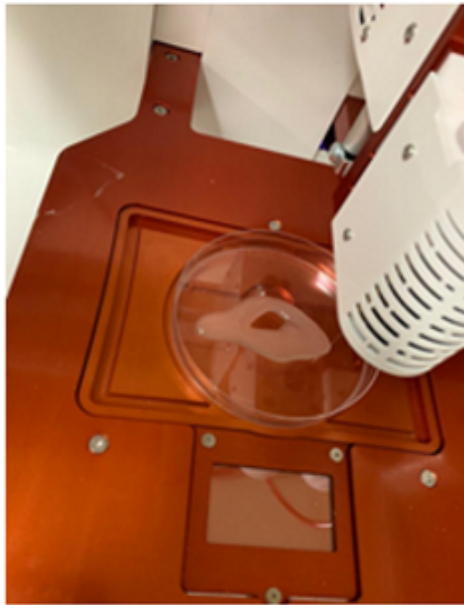
Printing parameters Evaluation by two-dimensional (2D) print testing.



(a)



(b)



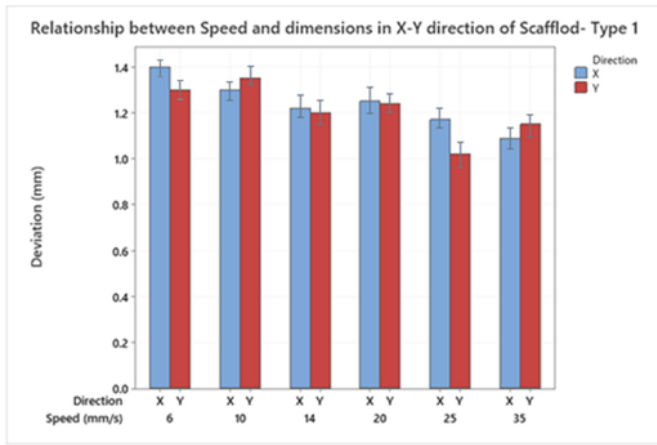
(c)



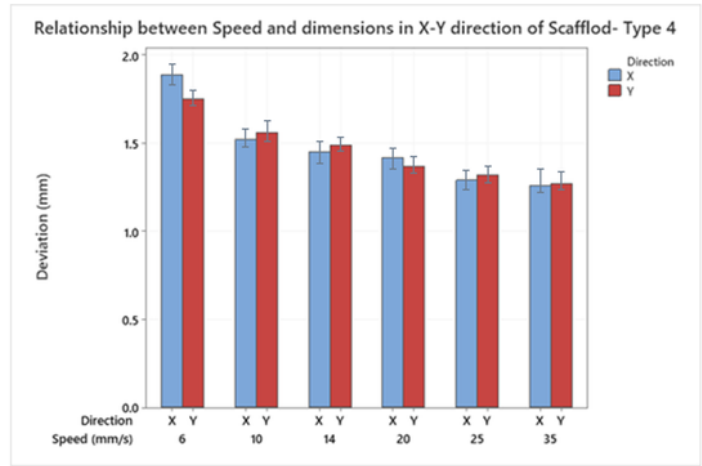
(d)

**Figure 8**

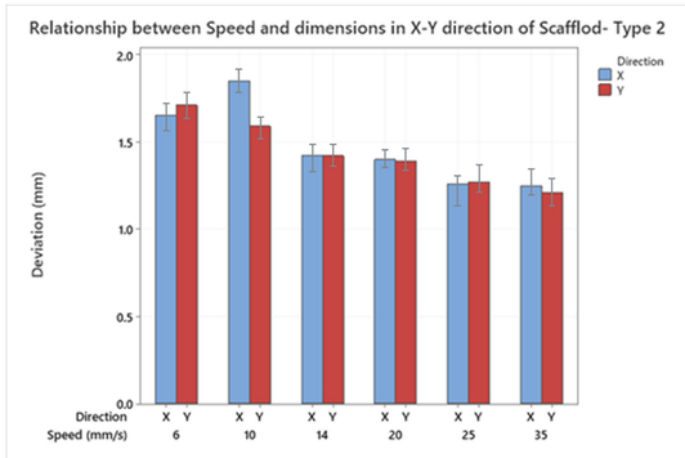
Printing parameters Evaluation by three-dimensional (3D) print testing.



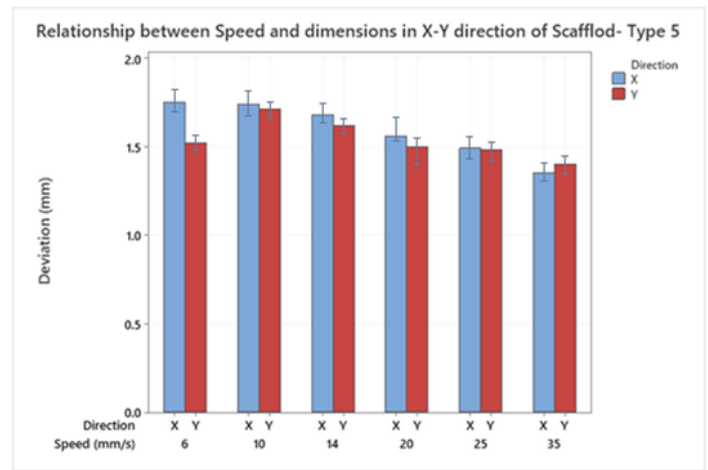
(a)



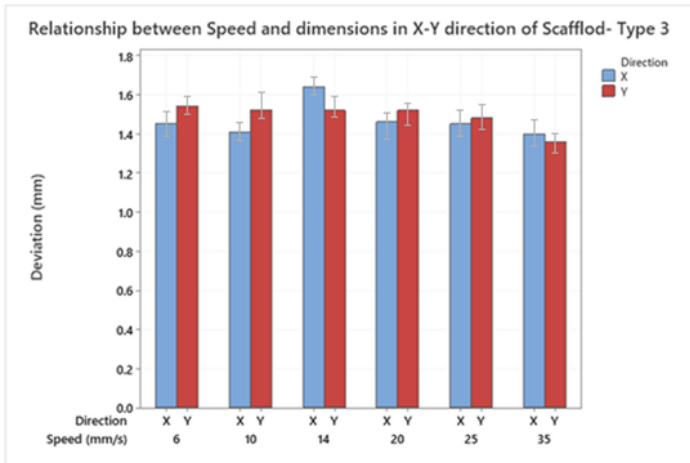
(d)



(b)



(e)



(c)



(f)

## Figure 9

Relationship between speed and dimensions in X-Y direction of Scaffold. (a) Type 1 (b) Type 2 (c) Type 3 (d) Type 4 (e) Type 5 (f) Type 6.